

Time Estimation of Topotecan Penetration in Retinoblastoma Cells Through Image Sequence Analysis

Debora Chan¹ , Ursula Winter² , Paula Schaiquevich², Rodrigo Ramele³ ,
and Juliana Gambini^{1,3,4}  

¹ Universidad Tecnológica Nacional, Regional Buenos Aires, Buenos Aires, Argentina
mchan@frba.utn.edu.ar

² CONICET - Hospital de Pediatría Prof. Dr. Juan P. Garrahan,
Buenos Aires, Argentina

³ Depto. de Ingeniería en Informática, Instituto Tecnológico de Buenos Aires,
Buenos Aires, Argentina
mgambini@itba.edu.ar

⁴ Depto. de Ingeniería en Computación,
UNTref, Buenos Aires, Pcia. de Buenos Aires, Argentina

Abstract. Retinoblastoma is the most common intraocular tumor in childhood. Topotecan has been widely used as an antineoplastic agent for retinoblastoma treatment. Topotecan penetration into living tumorspheres is quantified using confocal microscopy. This fluorescent drug dyes the living tissue and it can be recorded in a sequence of images over a period of time. The effective penetration of the drug depends on culture characteristics and requires a very specific timing. This penetration time is calculated empirically by an expert. The purpose of this work is to offer a statistical model to automatically estimate the penetration time of topotecan in the cell, based on the information obtained from a sequence of tumorsphere images.

Keywords: Sequence of confocal microscopy image ·
Statistical model · Tumorspheres · Retinoblastoma

1 Introduction

Retinoblastoma is the most frequent ocular tumor in childhood. It is characterized by the appearance of malignant cells in the retina. In Argentina, 45 new cases are detected per year, and 80% are referred for care to Prof. Dr. Juan Pedro Garrahan Hospital, Buenos Aires, where the current cure rate is over 98%. Worldwide, approximately 60% of cases of retinoblastoma occur unilaterally (only in one eye) while the remaining 40% compromises both eyes. In unilateral disease, the average age of onset in children is 2 years old, while in the bilateral case, it is 1 year old. For its treatment, Garrahan Hospital currently relies on a small number of drugs that are administered by different routes according to

the ophthalmologist's and oncologist's criteria, including: systemic (intravenous infusion), intravitreal and intra-arterial treatment. Each administration route has its advantages and disadvantages and the delivery of one treatment or the other depends on medical criterion. Local administration routes, such as intravitreal and intra-arterial routes have advantages over systemic chemoreduction, because they reduce the occurrence of serious adverse events such as severe myelosuppression [7, 11]. One of the drugs used in retinoblastoma treatment is topotecan.

Several authors have studied retinal diseases using different types of medical images and statistical modeling. For example in [9] a study for tumor classification using a probabilistic framework is presented. In [12] a method for vessel segmentation using active contours is introduced. In [6] a work focused on retinoblastoma detection is presented and several processing techniques are reviewed, all of them based on different types of medical image processing. In [10], the authors contribute to understanding retinoblastoma by studying drug penetration and response to chemotherapy to optimize patient treatment. Inspired by that work, in this paper we focus on image sequences analysis and processing techniques combined with statistical analysis, in order to determine the penetration time of topotecan in tumor clusters (set of tumor cells).

The objectives of this work are:

1. To estimate the time that topotecan consumes in penetrating the whole tumorsphere by means of microscopy image sequence analysis. The tumorsphere is considered to have been totally penetrated when it has a homogeneous color in the central region. We work with live-cell imaging.
2. To compare the penetration rate of topotecan between types of tumorspheres from Patient 1 and Patient 2.
3. To Compare the penetration rate of topotecan between different sizes of tumorspheres, derived from the same patient.

This article unfolds as follows. In Sect. 2.1, the experiment and image processing techniques to segment the microscopy image sequence are described. In Sect. 2.2, a statistical analysis of topotecan fluorescence evolution based on a mixed model with fixed and random effects is performed. Section 3 shows the results and a discussion. Finally, in Sect. 4, final remarks and future works are presented.

2 Materials and Methods

The experiment consists of the following steps: two primary cell cultures are obtained from the intraocular tumor of two patients, which were enucleated due to the advanced nature of the disease. After signing the informed consent (Protocol # 904, Hospital de Pediatria J. P. Garrahan), once the enucleation is completed by the ophthalmologist, she/he takes tumor samples, which are placed in the middle of defined cultures for primary cell cultures. Once the cultures are

established and characterized according to the morphology and cellular markers of the retina, they are used to study the penetration speed of the drug, for more details, see [10].

The main advantage of having chosen topotecan is that its penetration can be quantified through its fluorescence emission by laser excitation. The microscope used is Olympus Fluoview FV1000 confocal laser scanning microscope (Olympus, Tokyo, Japan) with imaging software (Olympus Fluoview FV10-ASW v1.7c) and equipped with a UPlanSApo 20X/0.75 NA objective.

The cell cultures studied belong to two patients:

- Patient 1: the patient was enucleated in the first line of treatment without having previously received chemotherapy.
- Patient 2: the patient had received chemotherapy prior to the enucleation of the affected eye.

Obtaining tumor cell primary cultures is an important challenge due to stringent growth and maintenance conditions. These patient models are unique in Argentina and given the aforementioned conditions, there is a limited number of available models. These cell cultures, to which we refer to as tumorspheres, are classified, according to their size, into three categories: small, medium and large. Then, $1\text{ }\mu\text{l}$ of a $10\text{ }\mu\text{g/ml}$ solution of topotecan is injected to the cell culture and a sequence of microscopy images are taken. The penetration time of the drug in the tumorsphere is expected to be predicted according to the fluorescence evolution over time. Figure 1 shows an example of a sequence of microscopy images corresponding to a large size tumorsphere from Patient 1. It can be observed that gray levels of pixels become brighter as time passes by. As topotecan penetrates the cell, it takes on brighter gray levels.

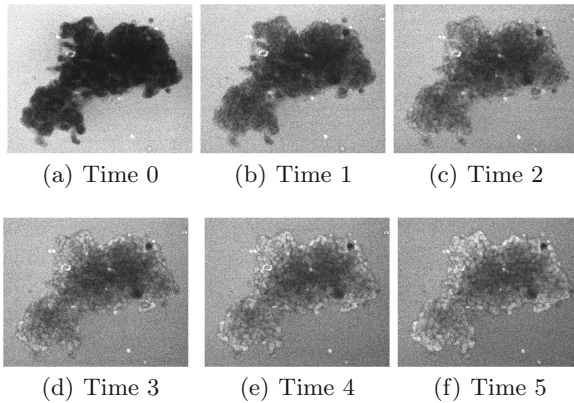


Fig. 1. Example of a sequence of microscopy images taken at 30 s intervals, corresponding to large size tumorsphere from Patient 1.

2.1 Image Sequence Analysis and Interpretation

In this section, the methods of image analysis used for automatic interpretation of a sequence of microscopy images are described.

The microscopy images are contaminated with noise which can be observed as a granulation. Figure 1 shows an example of a sequence of images where none image improvement technique was applied. Noise confuses automatic methods of image interpretation and it is necessary to eliminate it before starting the analysis. A method of noise removal with edge preservation called Anisotropic Diffusion method [5] is applied because it balances noise reduction, edge preservation and low computational cost [3]. Figure 2 shows the result of applying the method to the images of Fig. 1.

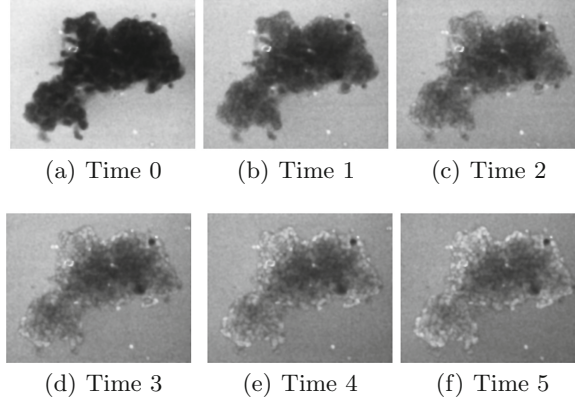


Fig. 2. Results of applying the Anisotropic Diffusion Method to the images of Fig. 1.

The main idea is to classify the pixels inside the tumorsphere in two classes, black and white. Black zones correspond to regions of the tumorsphere where topotecan did not penetrate. White zones correspond to regions of tumorspheres where topotecan penetrated. In order to classify the pixels inside the tumorsphere, the contour of the tumorsphere in the first image of the sequence is computed using an Active Contours algorithm, presented in [8]. This method was successfully modified for ultrasound image segmentation [2]. This procedure receives, as input data, an image I_1 , the first image of the sequence and an initial region inside the object of interest. Then, it returns a list of pixels belonging to the contour of the object of interest, named C . It has several advantages over other methods of active contours because rather than solving differential equations, the contour is found through y the interchange between two lists of neighboring pixels, saving computational cost. This method is highly efficient since it determines the contour of the object with high precision and it can be used in applications with real time requirements or constrained computational resources. Figure 3(a) shows the initial region of the algorithm, chosen in a supervised way. Figure 3(b) shows the computed contour for a small tumorsphere of Patient 1. Given the contour of the cell, the set of pixels in the inner of the contour, TS are computed.

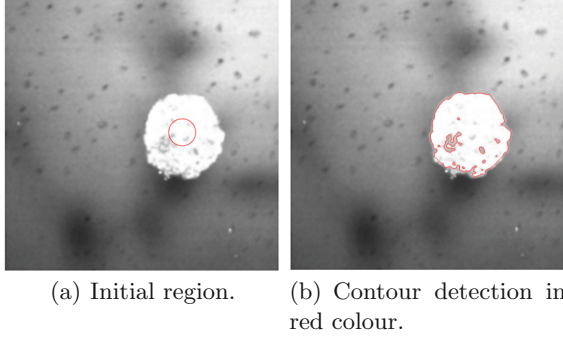


Fig. 3. Tumorsphere contour detection.

$$TS = \{(x, y) \in I / (x, y) \text{ is inside } C\} \quad (1)$$

Then, we calculate the threshold to segment TS in two classes, by means of Otsu's thresholding method [4], obtaining two colors for region TS in the image called B_1 . We use the same contour and the same threshold to analyze the entire sequence, obtaining $\{B_1, \dots, B_n\}$, where n is the number of sequence images. Results are presented in Fig. 4(a)–(f). The background is excluded from the analysis.

We calculate the percentage of black pixels within the tumorsphere. The percentage decreases as time passes by, indicating that the topotecan penetrates in the cell. Table 1 shows the results for each image of the sequence of Fig. 4.

The percentage of black pixels for each image of the sequence is computed as:

$$p_{Black}^j = \frac{\# \{(x, y) \in TS / B_j(x, y) = 0\}}{M}, \quad j = 1, \dots, n \quad (2)$$

where (x, y) is a pixel location and M is the total number of pixels of the object TS .

2.2 Statistical Analysis

In this section, a statistical model for time penetration prediction is performed using the results obtained in Sect. 2.1 for 11 tumorsphere samples from Patient 1 and 10 tumorsphere samples from Patient 2.

Generalized Mixed Models make it possible to predict the expected value of the response variable of the phenomena under study, considering the temporal variability and the correlation. With the mixed model both, fixed effects as tumorsphere sizes, and random effects, which are essential due to the biological variability between samples can be included in the same model [1]. In this case, the response variable is the penetration time, estimated from the black pixels rate.

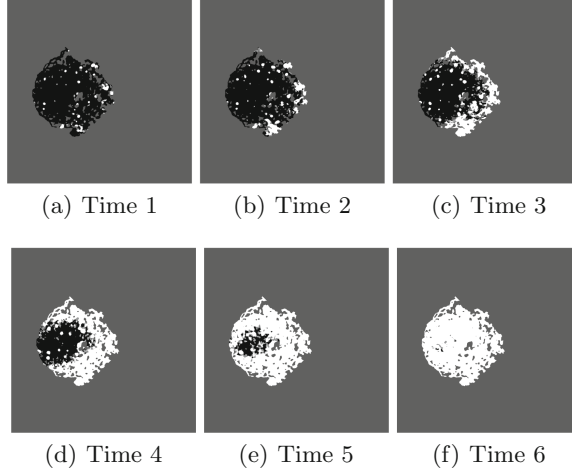


Fig. 4. Two-class tumorsphere classification.

Table 1. Percentage of black pixels within the tumorsphere for each image of the sequence of Fig. 4.

Image	Fig. 4(a)	Fig. 4(b)	Fig. 4(c)	Fig. 4(d)	Fig. 4(e)	Fig. 4(f)
p_{Black}	0.94%	0.87%	0.68%	0.39%	0.13%	0.005%

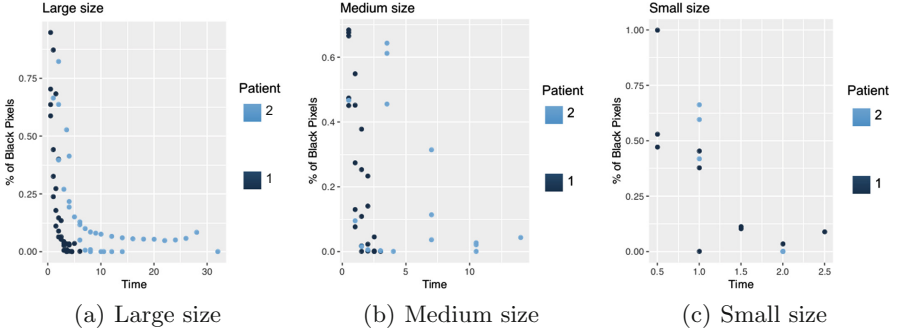


Fig. 5. Topotecan penetration evolution for different cell sizes.

Figure 5(a)–(c) show the evolution of the percentage of black pixels for both patients, for large, medium and small cells, respectively.

We propose the following statistical model

$$\hat{Y}_{ij} = a_i + \beta_0 t_{j(i)}^{\beta_i} e^{(\alpha_L * L + \alpha_S * S) t_{j(i)}}$$

where

- i number of patient, $i \in \{1, 2\}$.
- $\beta_0, a_i, \beta_i, i = 1, 2$ are the unknown coefficients.
- Y_{ij} varies from 0 to 1 and is the black pixel rate inside the cell at the $t_{j(i)}$ time, corresponding to the i -th patient, with $j \in \mathcal{N}$.
- $t_{j(i)}$ time in the j -th image of the sequence for patient i (1 or 2), whereas j is enclosed in parenthesis as a nested factor on i and references the time point in which the image was captured. This depends on each patient and each tumorsphere size.
- α_L and α_S coefficients correspond to Large and Small tumorspheres respectively.
- $L = 1$ if the size of the tumorsphere is large and $L = 0$ in other case. Likewise, $S = 1$ if the size of the tumorsphere is small and $S = 0$ in any other case. Hence, a middle-sized tumorsphere is identified when $L = 0$ and $S = 0$.

3 Results and Discussion

In this section, the results of the statistical model and a discussion is presented. Microscopy images were taken at 30 s for some sequences and at 60 seconds for others. For some of them, the penetration time reached 210 s for Small tumorspheres while it took almost 1920 s for their Large counterparts. Therefore, time varies from 30 s to 1920 s. Coefficients α_L and α_S take values 0 or 1.

Black pixel rate plotting shows different curves for each one of the tumorsphere sizes and is different for the two patients. However, both plots have a decreasing tendency for increased time values. For this reason, a Γ family distribution was selected, due to their versatility and their ability to capture the variability per patient and per tumorsphere size.

Considering size, average penetration times are 164.4 s (Big), 144.6 s (Medium) and 1.83 m (Small) for the previously untreated patient, whereas 8.66 m (Big), 8.3 m (Medium) and 109.8 s (Small) for the patient who underwent a previous treatment.

Concerning the penetration time based on tumorsphere size and patient, ANOVA testing shows that differences are statistically significant.

The estimated coefficients are given by:

- Patient 1:

$$\hat{Y}_{1j} = 0.3127 t_{j(1)}^{-0.251} e^{(0.0065 * L - 0.0923 * S) t_{j(1)}}$$

- Patient 2:

$$\hat{Y}_{2j} = 0.5018 t_{j(2)}^{-0.205} e^{(0.0065 * L - 0.0923 * S) t_{j(2)}}$$

For both models, all coefficients are statistically significant. The residuals are approximately Gaussian distributed. The Levene test does not reject the homoscedasticity assumption of the model in any case. With this model comparisons can be between large - medium size and small - medium size. For each of the sizes of tumorspheres and for each patient considered, it is possible to compute the average time at which the percentage of blacks is less than 10%. Due to space constraints final results are not presented.

4 Conclusions

This work shows that a statistically significant model can be devised in order to predict the required penetration time of topotecan in a tumorsphere, depending on the type of patient. The model proposed here can offer complementary information to care givers about the penetration time, which can be accurately estimated. The conclusion of the study indicates that the larger the size of the tumorsphere, the longer the penetration time. In addition, the penetration time is longer in tumorspheres corresponding to Patient 2 than those corresponding to Patient 1. This result is not surprising as larger seeds consist of a greater number of cells arranged in multilayers around a central core. Therefore, spheres are not mere aggregates of cells but 3D structures that may hamper drug accessibility.

As future work, additional work should be conducted in order to verify alternative statistical models and to use neural networks to estimate penetration time.

Conflict of Interest. The authors declare that they have no conflict of interest.

References

1. Bates, D., Mächler, M., Bolker, B., Walker, S: Fitting linear mixed-effects models using lme4. arXiv preprint [arXiv:1406.5823](https://arxiv.org/abs/1406.5823) (2014)
2. Bisso, I., Gambini, J.: Ultrasound image segmentation through a fast active contour based algorithm. In: VI Congreso Latinoamericano de Ingeniería Biomédica (2014). https://doi.org/10.1007/978-3-319-13117-7_92
3. Haider, S.A., Cameron, A., Siva, P., Lui, D., Shafiee, M.J., Boroomand, A., Haider, N., Wong, A.: Fluorescence microscopy image noise reduction using a stochastically-connected random field model. Nature Scientific report, vol. 6, p. 20640 (2016). <https://doi.org/10.1038/srep20640>
4. Otsu, N.: A threshold selection method from gray-level histogram. IEEE Trans. Syst. Man Cybern. **9**, 62–66 (1979). <https://doi.org/10.1109/TSMC.1979.4310076>
5. Perona, P., Malik, J.: Scale-space and edge detection using anisotropic diffusion. IEEE Trans. Pattern Anal. Mach. Intell. **12**(7), 629–639 (1990). <https://doi.org/10.1109/34.56205>
6. Sadhana, S., Mallika, D.: A review of retina blood vessel detection using image segmentation techniques. Int. J. Innovative Res. Sci. Technol. **3**, 247–253 (2017)
7. Schaiquevich, P., Ceciliano, A., Millan, N., Taich, P., Villasante, F., Fandino, A.C., Dominguez, J., Chantada, G.L.: Intra-arterial chemotherapy is more effective than sequential periocular and intravenous chemotherapy as salvage treatment for relapsed retinoblastoma. Pediatr. Blood Cancer, 766–770 (2013). <https://doi.org/10.1002/pbc.24356>
8. Shi, Y.G., Karl, W.C.: A real-time algorithm for the approximation of level-set-based curve evolution. Image Process. **17**(5), 645–656 (2008). <https://doi.org/10.1109/TIP.2008.920737>
9. Tobin, K.W., Abdelrahman, M., Chaum, E., Govindasamy, V.P., Karnowski, T.P.: A probabilistic framework for content-based diagnosis of retinal disease. In: 29th Annual International Conference of the IEEE Engineering in Medicine and Biology Society, pp. 6743–6746 (2007). <https://doi.org/10.1109/IEMBS.2007.4353909>

10. Winter, U., Aschero, R., Fuentes, F., Buontempo, F., Zugbi, S., Sgroi, M., Sampor, C., Abramson, D., Carcaboso, A., Schaiquevich, P.: Tridimensional retinoblastoma cultures as vitreous seeds models for live-cell imaging of chemotherapy penetration. *Int. J. Mol. Sci.* **20**, 1077 (2019). <https://doi.org/10.3390/ijms20051077>
11. Winter, U., Nicolas, M., Sgroi, M., Sampor, C., Torbidoni, A., FandiOo, A., Chantada, G., Munier, F., Schaiquevich, P.: Assessment of retinoblastoma rna reflux after intravitreal injection of melphalan. *Br. J. Ophthalmol.* **3**, 415–418 (2018). <https://doi.org/10.1136/bjophthalmol-2017-310574>
12. Zhao, Y., Rada, L., Chen, K., Harding, S.P., Zheng, Y.: Automated vessel segmentation using infinite perimeter active contour model with hybrid region information with application to retinal images. *IEEE Trans. Med. Imaging* **34**(9), 1797–1807 (2015). <https://doi.org/10.1109/TMI.2015.2409024>